www.czasopisma.pan.pl PAN POLSKA AKADEMIA NAUK www.journals.pan.pl

PAN ARCHIVES OF ACOUSTICS
Vol. 41, No. 1, pp. 139–150 (2016)

DOI: 10.1515/aoa-2016-0014

Digital Synthesis of Sound Generated by Tibetan Bowls and Bells

Andrzej GOŁAŚ, Roman FILIPEK

Faculty of Mechanical Engineering and Robotics
AGH University of Science and Technology
Al. A. Mickiewicza 30, 30-059 Kraków, Poland; e-mail: romanf@agh.edu.pl

(*received October 24, 2011; accepted April 2, 2012*)

The aim of this paper is to present methods of digitally synthesising the sound generated by vibroacoustic systems with distributed parameters. A general algorithm was developed to synthesise the sounds of selected musical instruments with an axisymmetrical shape and impact excitation, i.e., Tibetan bowls and bells. A coupled mechanical-acoustic field described by partial differential equations was discretized by using the Finite Element Method (FEM) implemented in the ANSYS package. The presented synthesis method is original due to the fact that the determination of the system response in the time domain to the pulse (impact) excitation is based on the numerical calculation of the convolution of the forcing function and impulse response of the system. This was calculated as an inverse Fourier transform of the system's spectral transfer function. The synthesiser allows for obtaining a sound signal with the assumed, expected parameters by tuning the resonance frequencies which exist in the spectrum of the generated sound. This is accomplished, basing on the Design of Experiment (DOE) theory, by creating a meta-model which contains information on its response surfaces regarding the influence of the design parameters. The synthesis resulted in a sound pressure signal in selected points in space surrounding the instrument which is consistent with the signal generated by the actual instruments, and the results obtained can improve them.

Keywords: sound synthesis; coupled fields; FEM; DOE; response surface methodology.

1. Introduction

A synthesis of sound using digital models of vibroacoustic systems was conducted for selected musical instruments – Tibetan bowls and bells. These instruments, from the group of idiophones, were chosen due to their unique axisymmetrical shape, which has evolved into its current state over the years, as well as due to how their vibration is caused by impact. The differences between them related to the curvature of the surface as well as wall thickness, causing them to have varying proportions between the resonance frequencies contained in the sound spectrum. The desired proportions between frequencies are determined based on experiments conducted for the first time in the 6th century BC by Pythagoras (Fauvel *et al.*, 2006), the aim of which was to explain why consecutive or harmonising sounds created while playing a musical instrument result in their consonant or dissonant perception by the listener. It is worth noting that while analysing the results, Pythagoras did not concern himself with the concept of frequencies; instead, using geometrical proportions, e.g., the length of a monochord string being shortened. He deducted that consecutive sounds are pleasant to the listener if the string length follows proportions outlined by fractions consisting of small integer numbers. This allowed for creation of guidelines for the first musical scale – a set of given proportions between sound frequencies, called intervals. In the recent years, the explanation for the phenomenon of consonance and dissonance is based on the nonlinear dynamics of auditory perception with a scheme of mutually coupled oscillators (Lots, Stone, 2008).

Tibetan bowls, also known as *singing bowls*, are designed and created in accordance with tradition in many Asian countries. There are two methods of enforcing the vibrations of Tibetan bowls. One of them involves using a wooden cylinder held in one's hand to hit the edge or side area of the bowl, which results in an impulsive sound. The second method, which will not be taken into account in this work, involved dragging the cylinder over the perimeter of the bowl, which, due to friction, results in forcing vibrations and a constant *singing* sound. Dynamic tests of selected bowls

using both methods were conducted (Inácio, Henrique, 2006). The model used by the authors does not take into account the coupling of the structural vibrations with the acoustic field, although the assessment of the model parameters was carried out based on acoustic readings. The consecutive proportions between the first five component frequencies of the spectrum and the first frequency fall between 2.7–2.9, 4.8–5.7, 7.5–9.1, 10.6–13.1. The dynamic behaviour of the surface of the bowl after filling it with water was researched (Terwagne, Bush, 2011), though in the context of phenomena occurring in the fluid rather than of assessing the acoustic pressure.

The second group of instruments used in the synthesis are bells. One of the oldest known types of bells are Chinese bells (Chih-Wei *et al.*, 2013) which generate a sound with two basic component tones due to their oval shape. In the Western culture, the bells that became common during the Middle Ages were in the shape of a tulip (Fletcher, Rossing, 1998). The frequencies of the vibrations of a bell obtained during the casting process are usually additionally tuned by choosing the proper material of the inside surface of the bell, which is very important in the case of bells in chimes (Sankiewicz *et al.*, 1994, Budzyński, Sankiewicz, 2000). The first resonance frequency in the sound spectrum of bells is called a *hum* and usually does not stand out. The tone height perceived by the listener is influenced by the following resonance frequencies appearing in the sound spectrum, named after their characteristic intervals: *prime*, *minor third*, *fifth*, and *octave* (Fletcher, Rossing, 1998). What makes the timbre of the bell special is the third and prime frequency between which the *minor third* interval happens. Research was carried out in order to change this interval into a *major third* (Lehr, 1987) which resulted in bells with a new shape obtained by building and optimising the model created by using the finite element method (FEM). Researchers from *Australian Bell* (McLachlan, Keramati, 2003) elaborated on this and designed many more shapes of bells optimising them by analysing the sensitivity of node displacement in the FEM model in order to only generate circular vibrations that allowed *truly harmonic* bells to exist, for which the first seven components are fifth and octave intervals.

Tuning of the frequencies is done by Design of Experiments (DOE) and Response Surface (RS) methods (Mańczak, 1978; Myers, Montgomery, 2004; Jiju, 2014). When it comes to bowl construction, the scope of proportions between resonance frequencies in a spectrum is wide. This is related to the consistent thickness and almost elliptic shape of the bowl. This means a perfect tuning of the component frequencies of the spectrum to the frequencies of specific musical intervals. A compromise has to be made, as correcting the proportions between any given frequencies worsens the proportions of others. Although, fine tuning the frequencies of bells is possible due to their hyperbolic surface shape and varying thickness.

Sound synthesis methods are divided (Bilbao, 2009) into two basic groups: abstract and physical. The earliest work related to abstract sound synthesis started in the late 50s in the 20th century at Bell Laboratories. It involved methods such as *additive synthesis*, which was based on summation of sinusoidal signals, *subtractive* – based on generating an input signal, e.g., white noise, and modifying it by filtering, or *AM* and *FM synthesis* – based on amplitude modulation or frequency of sinusoidal signals. An advantage of these methods is the possibility of applying them in real time with a relatively low processing power. The disadvantages are low audio quality and an unnatural tone (Bilbao, 2009). In physical model methods, the basis consists of a mathematical description of the physical system (the instrument). It takes the form of partial differential equations describing vibrations of the strings, the surface, or changes in acoustic pressure. Historically, the first method was the use of *lumped mass–spring networks* (Cadoz *et al.*, 1983), in which connected networks with lumped parameters (mass and spring) describe, e.g., string vibration in 1D and membrane vibration in 2D. Another method used a modal synthesis in which the natural frequencies and mode shapes are both obtained for the differential equations describing the system, followed by receiving the system response by use of modal superposition (Ren *et al.*, 2013). Another important synthesis method is the *digital waveguides* method as presented in a very computationally effective way by Julius Smith (Smith, 1992). He proposed an algorithm for one-dimensional acoustic systems described with a wave equation (Rossing, 2007), in which vibrations are modelled as two travelling waves not affecting each other, and digital synthesis is performed by using two delay lines, which is very effective computationally. This idea was then expanded by the creation of complex structures consisting of networks of delay lines in different configurations (Bilbao, 2009; Czyżewski *et al.*, 2002, 1996).

In methods of direct numerical simulation, obtaining an analytical solution for an acoustic wave equation is possible for multiple systems (Rdzanek, 2011), although it requires simplification regarding the shape of the area in question, especially the fragment of the boundary which defines the source of sound. For the purposes of acoustic field modelling in systems with advanced geometry, numerical methods are used (Gołaś, 1995), such as the finite difference method (FDM), the boundary element method (BEM) (Dobrucki, Bolejko, 2006; Nowak, Zieliński, 2015), or FEM (Filipek, Wiciak, 2005; 2008). The mathematical model of the system used for the presented sound synthesis was created by using FEM, and it takes into ac-

count the coupling between vibrations of the structure and the acoustic medium surrounding it.

2. Sound synthesis method

Digital sound synthesis takes place in a numerical synthesiser presented in Fig. 1, which consists of two main blocks. The task of the first block is to indicate structural parameters allowing the generated sound to fulfil the expected acoustic parameters. They are the component frequencies of the spectrum of generated sound and the appropriate proportions between them. A meta-model is created based on the DOE method that contains the structural parameters and their influence on the acoustic signal spectrum. It allows to introduce restrictions based on the expected proportions between the component frequencies of the spectrum and to find the structural parameters that allow to match these proportions.

The second block depicted in Fig. 1. Sound synthesis takes place in specific points of the field based on the resulting from meta-model parameters. By using FEM, a complex model is created that describes the mechanical and acoustic fields and takes into account the coupling between them. Next, based on the resulting steady-state characteristics of the vibroacoustic system, the acoustic pressure signal is generated. For linear, time invariant systems, as the system considered in this study, transfer function $G(\omega)$ between system input $X(\omega)$ and output $Y(\omega)$ may be defined in frequency domain as:

$$G(\omega) = \frac{Y(\omega)}{X(\omega)}. \tag{1}$$

When the system input in the time domain is assumed as Dirac delta:

$$\delta(t) = \begin{cases} \infty, & t = 0, \\ 0, & t \neq 0. \end{cases} \tag{2}$$

Laplace transform of the input $x(t)$ is equal to unity ($X(\omega) = 1$) and it ensures that the equation $Y(\omega) = G(\omega)$ is fulfilled. The system impulse response $g(t)$ is calculated then by inverse Fourier transform (Zieliński, 2005) of system's transfer function:

$$g(t) = F^{-1}(G(j\omega)). \tag{3}$$

The system response $y(t)$ for any excitation may be calculated as a convolution:

$$y(t) = g(t) * x(t), \tag{4}$$

where $x(t)$ is a forcing signal and $g(t)$ is an impulse response.

2.1. Mathematical model of coupled mechanical and acoustic field

The key element of the synthesis algorithm is modelling of the mechanical and acoustic field and the coupling between them. Since the mechanical field at all points with coordinates x_i in domain Ω_S is described by displacements u_i, equilibrium equations (balance of the linear momentum) are given in the index form as:

$$\rho \frac{\partial^2 u_i}{\partial t^2} + \mu \frac{\partial u_i}{\partial t} - \sigma_{ji,j} - b_i = 0, \qquad i,j = 1,2,3, \tag{5}$$

where ρ is mass density, μ is damping coefficient, $\sigma_{ji,j}$ are components of Cauchy stress tensor, b_i are body

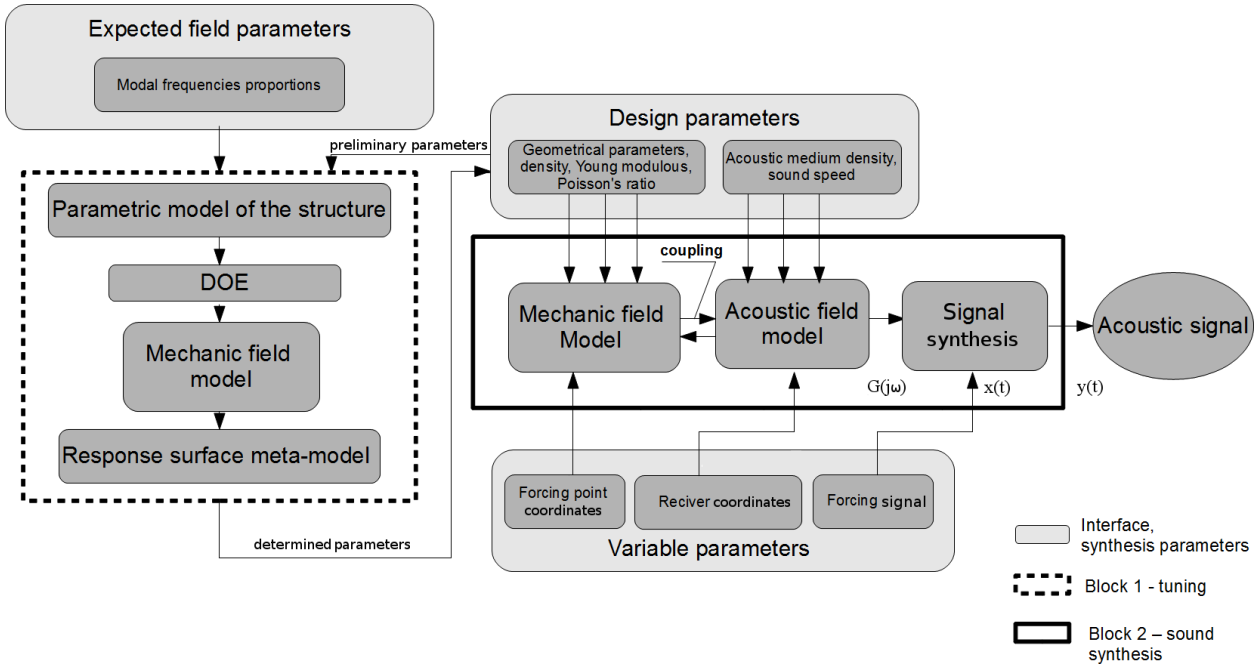

Fig. 1. Sound synthesis flowchart.

force components. Boundary conditions can be given as stress conditions on $\partial_t \Gamma_S$ by the traction condition or as displacement conditions on $\partial_u \Gamma_S$:

$$(\sigma_{ij} n_j)|_{\partial_t \Gamma_S} = \overline{t_i}, \tag{6}$$

$$(u_i)|_{\partial_u \Gamma_S} = \overline{u}_i. \tag{7}$$

In the case of linear elasticity, the stress components are given by stress-strain relations as:

$$\sigma_{ij} = D_{ijkl} \varepsilon_{kl}, \tag{8}$$

where ϵ_{kl} are strains and D_{ijkl} are constitutive matrix components. The properties of isotropic materials are defined by two parameters: Young modulus E and Poisson ratio ν:

$$D_{ijkl} = \frac{E}{2(1+\nu)} (\delta_{il}\delta_{jk} + \delta_{ik}\delta_{jl}) + \frac{E\nu}{(1+\nu)(1-2\nu)} \delta_{ij}\delta_{kl}, \tag{9}$$

where δ_{ij} is Kronecker symbol, and $\delta_{ij} = 0$ for $i \neq j$, and $\delta_{ij} = 1$ for $i = j$. In the Cartesian tensor form virtual strains are related to virtual displacements as:

$$\delta\varepsilon_{ij} = \frac{1}{2} (\delta u_{i,j} + \delta u_{j,i}). \tag{10}$$

An integral, variational form of Eq. (5) may be written as:

$$\int_{\Omega_S} \delta u_i \rho \frac{\partial^2 u_i}{\partial t^2} \, \mathrm{d}\Omega + \int_{\Omega_S} \delta u_i \mu \frac{\partial u_i}{\partial t} \, \mathrm{d}\Omega + \int_{\Omega_S} \delta\varepsilon_{ij}\sigma_{ij} \, \mathrm{d}\Omega - \int_{\Omega_S} \delta u_i b_i \, \mathrm{d}\Omega - \int_{\Gamma_S} \delta u_i \overline{t_i} \, \mathrm{d}\Gamma = 0. \tag{11}$$

After finite element procedures (Zienkiewicz, Taylor, 2000), when using Galerkin method, Eq. (11) is given by:

$$\mathbf{M}_S \ddot{\mathbf{u}}_e + \mathbf{C}_S \dot{\mathbf{u}}_e + \mathbf{K}_S \mathbf{u}_e = \mathbf{f}_S, \tag{12}$$

where $\mathbf{M}_S$, $\mathbf{C}_S$, $\mathbf{K}_S$ are respectively mass, damping and stiffness matrix, $\ddot{\mathbf{u}}_e$, $\dot{\mathbf{u}}$, $\mathbf{u}_e$ are vectors of nodal acceleration, velocity, and displacement, while $\mathbf{f}_S$ is the forcing vector.

Natural frequencies of the system with the absence of damping are calculated with the assumption of harmonic displacements $\mathbf{u}_e = Re\left(\widetilde{\mathbf{u}}_e e^{j\boldsymbol{\omega} t}\right)$ where ω is the angular frequency and $\widetilde{\mathbf{u}}_e$ is the complex amplitude. It leads to the equation given by:

$$\left(-\omega^2 \mathbf{M}_S + \mathbf{K}_S\right) \widetilde{\mathbf{u}}_e = 0. \tag{13}$$

System natural frequencies and mode shapes correspond to eigenvalues and eigenvectors of the Eq. (13) and are calculated with the Lanczos method. The mathematical description of the acoustic field is derived from the Navier-Stokes equations of fluid momentum and the flow continuity equation with the assumption that fluid is compressible and there is no mean flow of the fluid. The resulting acoustic wave equation is given by:

$$\frac{1}{\rho_0 c^2} \frac{\partial^2 p}{\partial t^2} - \nabla \cdot \left(\frac{1}{\rho_0} \nabla p\right) = 0, \tag{14}$$

where p is the acoustic pressure, ρ_0 is the mean fluid density, and c is the speed of sound. The finite element formulation is obtained using the Galerkin procedure by testing wave Eq. (10) with a test function δp and integrating over the volume of the domain Ω_F:

$$\int_{\Omega_F} \delta p \frac{1}{\rho_0 c} \frac{\partial^2 p}{\partial t^2} \, \mathrm{d}\Omega + \int_{\Omega_F} \nabla\delta p \left(\frac{1}{\rho_0} \nabla p\right) \mathrm{d}\Omega - \int_{\Gamma_F} \delta p \frac{1}{\rho_0} \widehat{n} \nabla p \, \mathrm{d}\Gamma = 0, \tag{15}$$

where $d\Omega$ is the volume differential of the acoustic domain Ω_F, $d\Gamma$ is the surface differential of the acoustic domain boundary Γ_F, and $\widehat{n}$ is the unit vector normal to the boundary Γ_F. For the fluid structure coupling, there are crucial boundary conditions on the interface surface. From the equation of momentum conservation, the normal velocity on the boundary of the acoustic domain is given by:

$$\frac{\partial v_{n,F}}{\partial t} = -\frac{1}{\rho_0} \widehat{n} \cdot \nabla p. \tag{16}$$

Substituting (16) with (15) yields the form of (14), given by:

$$\int_{\Omega_F} \delta p \frac{1}{\rho_0 c} \frac{\partial^2 p}{\partial t^2} \, \mathrm{d}\Omega + \int_{\Omega_F} \nabla\delta p \left(\frac{1}{\rho_0} \nabla p\right) \mathrm{d}\Omega - \int_{\Gamma_F} \delta p \frac{\partial v_{n,F}}{\partial t} \, \mathrm{d}\Gamma = 0 \tag{17}$$

The normal acceleration of the fluid particle can be presented using the normal displacement of the fluid particle $\mathbf{u}_F$:

$$\widehat{n} \nabla p = -\rho_0 \widehat{n} \frac{\partial^2 \mathbf{u}_F}{\partial t^2}. \tag{18}$$

Substitution of (18) with (17) leads to:

$$\int_{\Omega_F} \delta p \frac{1}{\rho_0 c} \frac{\partial^2 p}{\partial t^2} \, \mathrm{d}\Omega + \int_{\Omega_F} \nabla\delta p \left(\frac{1}{\rho_0} \nabla p\right) \mathrm{d}\Omega + \int_{\Gamma_F} \delta p \frac{\partial^2 \mathbf{u}_F}{\partial t^2} \, \mathrm{d}\Gamma = 0. \tag{19}$$

Equation (19) after the FEM procedure (Zienkiewicz, Taylor, 2000) may be written as:

$$\mathbf{M}_F\ddot{\mathbf{p}}_e + \mathbf{K}_F\mathbf{p}_e + \rho_0\mathbf{R}\ddot{\mathbf{u}}_e = 0, \tag{20}$$

where $\mathbf{M}_F$, $\mathbf{K}_F$ are matrices of the medium's masses and stiffness, respectively, ρ_0 is the medium density, $\mathbf{R}$ is the coupling matrix, $\ddot{\mathbf{u}}_e$ is the vector of normal accelerations to the boundary surface. The coupling conditions on the interface between the acoustic fluid and the structure are given by:

$$\overline{\overline{\sigma}}\hat{n} + p\hat{n} = 0, \tag{21}$$

$$\hat{n}\cdot\mathbf{u}_S - \hat{n}\cdot\mathbf{u}_F = 0, \tag{22}$$

where $\overline{\overline{\sigma}}$ is the stress tensor on the boundary of the structure, p is the acoustic pressure, $\mathbf{u}_S$, $\mathbf{u}_F$ are the displacement vectors of the structure and fluid, respectively. Conditions (21)–(22) allow the calculation of pressure forces $\mathbf{f}_e^{pr}$ originating from acting of the fluid on the structure surface. After substitution of $\mathbf{f}_S = \mathbf{f} + \mathbf{f}_e^{pr}$ the equation (12) is given as:

$$\mathbf{M}_S\ddot{\mathbf{u}}_e + \mathbf{C}_S\dot{\mathbf{u}}_e + \mathbf{K}_S\mathbf{u}_e - \mathbf{R}\mathbf{p}_e = \mathbf{f}. \tag{23}$$

Equations (20) and (23) describe the complete finite element discretized equations for the fluid-structure interaction problem. These equations are written in an assembled form as:

$$\begin{bmatrix}\mathbf{M}_S & 0\\ \rho_0\mathbf{R} & \mathbf{M}_F\end{bmatrix}\begin{bmatrix}\ddot{\mathbf{u}}_e\\ \ddot{\mathbf{p}}_e\end{bmatrix} + \begin{bmatrix}\mathbf{C}_S & 0\\ 0 & 0\end{bmatrix}\begin{bmatrix}\dot{\mathbf{u}}_e\\ \dot{\mathbf{p}}_e\end{bmatrix} + \begin{bmatrix}\mathbf{K}_S & -\mathbf{R}\\ 0 & \mathbf{K}_F\end{bmatrix}\begin{bmatrix}\mathbf{u}_e\\ \mathbf{p}_e\end{bmatrix} = \begin{bmatrix}\mathbf{f}\\ 0\end{bmatrix}. \tag{24}$$

In a steady-state conditions and with the assumption of a harmonic excitation with the angular frequency ω and amplitude $\widetilde{\mathbf{f}}$, $\widetilde{\mathbf{u}}_e$, $\widetilde{\mathbf{p}}_e$ as $\mathbf{f} = \mathrm{Re}\left(\widetilde{\mathbf{f}}e^{j\omega t}\right)$, $\mathbf{u}_e = \mathrm{Re}\left(\widetilde{\mathbf{u}}_e e^{j\omega t}\right)$, $\mathbf{p}_e = \mathrm{Re}\left(\widetilde{\mathbf{p}}_e e^{j\omega t}\right)$, differential Eq. (24) are given as algebraic equations:

$$\left(-\omega^2\begin{bmatrix}\mathbf{M}_S & 0\\ \rho_0\mathbf{R} & \mathbf{M}_F\end{bmatrix} + j\omega\begin{bmatrix}\mathbf{C}_S & 0\\ 0 & 0\end{bmatrix} + \begin{bmatrix}\mathbf{K}_S & -\mathbf{R}\\ 0 & \mathbf{K}_F\end{bmatrix}\right) \cdot \begin{bmatrix}\widetilde{\mathbf{u}}_e\\ \widetilde{\mathbf{p}}_e\end{bmatrix} = \begin{bmatrix}\widetilde{\mathbf{f}}\\ 0\end{bmatrix}. \tag{25}$$

After defining the boundary conditions, it is possible to solve Eq. (25) by solving a system of linear algebraic equations with a proper numerical method.

3. Bowl and bell sound synthesis

The mathematical models allowing for assessing frequencies of the natural vibrations of systems were created with the use of the FEM implemented in the ANSYS Workbench suite. The objects studied first were Tibetan bowls. Two distinct shapes of Tibetan bowls were studied, the basic geometric parameters of which were measured for actual structures and presented in Table 1. To ensure further alteration, a parametric geometric model of both shapes was created (Fig. 2a). The shape of the bowl was defined by using a line profile rotated about its axis. The profile consisted of two curves linked by a connection clause. The first one described the base of the bowl and was a sector of an ellipse with eccentrics at 0.1 m horizontally, 0.025 m vertically. The second one described the side wall and was established as a circular segment with a radius of R. The following parameters defined the edge of the bowl: rg – radius of edge, h – height of bowl.

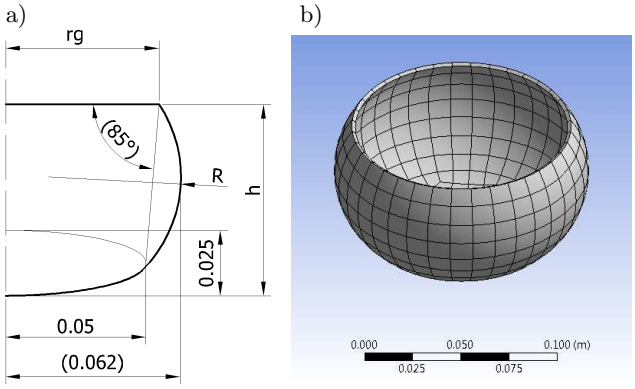

Fig. 2. Model of the bowl: a) model shape described with parameters: R – radius of side wall, rg – radius of bowl edge, h – bowl height, b) finite element mesh.

Next, the resulting surface was discretized (Fig. 2b) by use of Shell281 elements with a constant thickness g. Shell281 elements were chosen due to the fact that they are suitable for modelling thin coated structures and consist of eight nodes, being described by parabolic shape functions. The material parameters were established to be similar to the parameters of brass – Young's modulus E, density ρ, Poisson's coefficient ν, the values of which, alongside with varying geometric parameters, were summarized in Table 1.

Table 1. Defined material and geometric parameters.

Bowl no.	Young mod.	Density	Poisson ratio	Geometrical parameters			
	E [GPa]	ρ [kg·m^{-3}]	ν	h [m]	r [m]	rg [m]	g [m]
1	1.05	8600	0.34	0.070	0.045	0.055	0.0011
2				0.075	0.300	0.067	0.0023

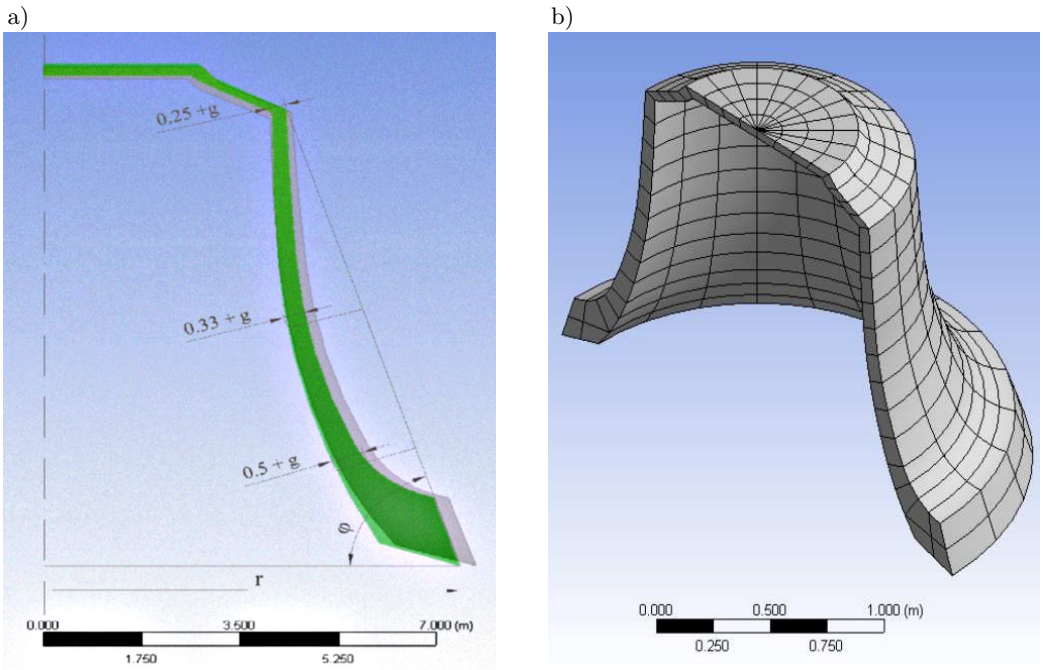

Fig. 3. Model of the bell: a) parametric geometry cross-section, b) finite element mesh.

The size of the elements was selected based on a grid independence analysis which showed that an element edge length of 0.02 m is enough. This results in a model consisting of approximately 200 elements and 700 nodes.

Bells were the second object of study. Sound synthesis was carried out for the Sigismund Bell in the Wawel Cathedral, which weighs 9650 kg with the diameter of 2.42 m. A parametric geometric model was created with the profile as shown in Fig. 7a. The exact shape of the profile was derived from the German bell-foundry tradition (Gołaś, Filipek, 2009). When it comes to geometry-defining parameters (Fig. 3a), those with a relative wall thickness – g, angle of the profile lean – φ, relative base radius – r, were chosen. Every change of the r parameter resulted in a rescaling of the geometry in such a way as to retain the constant diameter of the base of the bell. Twenty-node Solid186 solid elements were used to create the mathematical model of the bell. A half of the resulting mesh is presented in Fig. 3b and the full model contains approximately 750 elements and 5000 nodes.

Table 2. Defined material and geometric parameters.

	No.	Measured freq. [Hz]	Model freq. [Hz]	Difference [%]	Frequency proportions	
					ideal	obtained
Bowl No. 1	1	472.0	480.4	−1.79	–	1.00
	2	1329.0	1330.2	−0.09	–	2.77
	3	2448.0	2416.8	1.27	–	5.03
	4	3738.0	3678.6	1.59	–	7.66
	5	5165.0	5094.3	1.37	–	10.60
Bowl No. 2	1	334.0	321.1	3.86	–	1.00
	2	806.0	811.0	−0.63	–	2.53
	3	1488.0	1480.7	0.49	–	4.61
	4	2352.0	2328.9	0.98	–	7.25
	5	3356.0	3351.1	0.15	–	10.44
Sigismund Bell	1	91.0	92.3	1.41	1	1.00
	2	203.0	205.7	1.33	2	2.23
	3	230.0	232.8	1.19	2.4	2.52
	4	277.0	275.2	−0.64	3	2.98
	5	382.0	381.2	−0.22	4	4.13

3.1. Modal frequencies determination and system parameters tuning

The first phase of the study involved the designation of modal frequencies based on equation (13) as well as mode shapes with parameters corresponding to the actual models. The natural frequencies of the bowls and the bell indicated in the experiment were compared in Table 2 with the measured resonance frequencies of the actual structures. The measurement consisted of a frequency analysis of the acceleration and acoustic pressure signal recorded with the use of a data acquisition system (Filipek, 2013). The first four mode shapes were compiled for bowl no. 1 in Fig. 4 and for the bell in Fig. 5. The comparison between the vibrations of the bowls and the bell suggest that the hyperboloidal bell surface shape causes the mode with

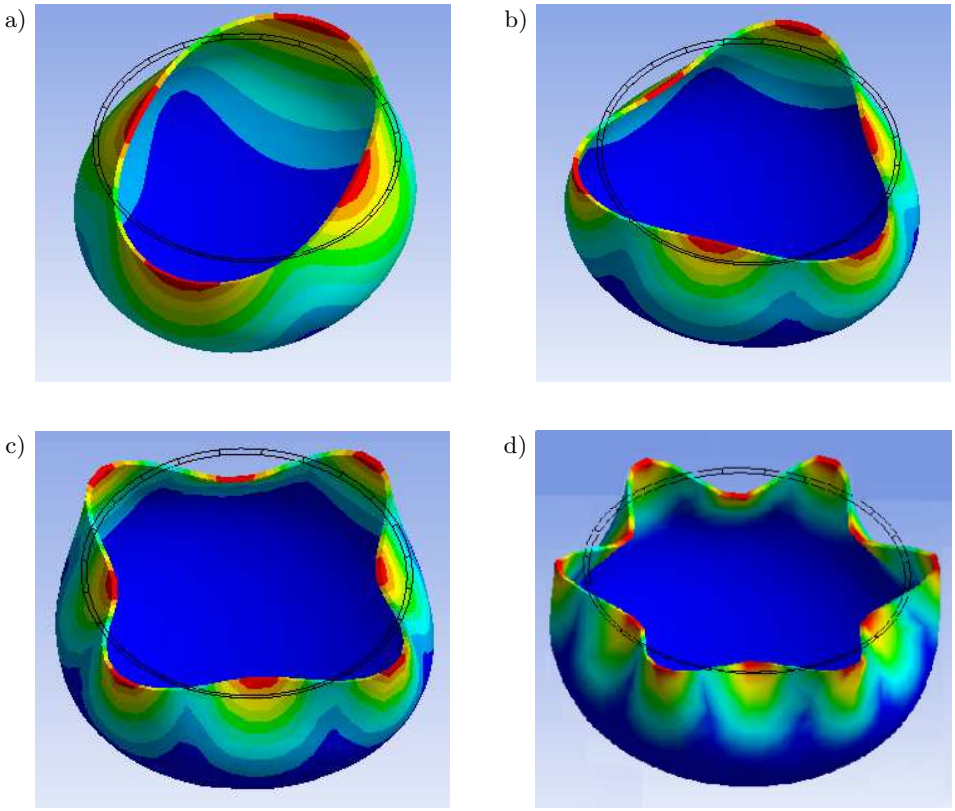

Fig. 4. Tibetan bowl mode shapes: a) first (2,0), b) second (3,0), c) third (4,0), d) fourth (4,0).

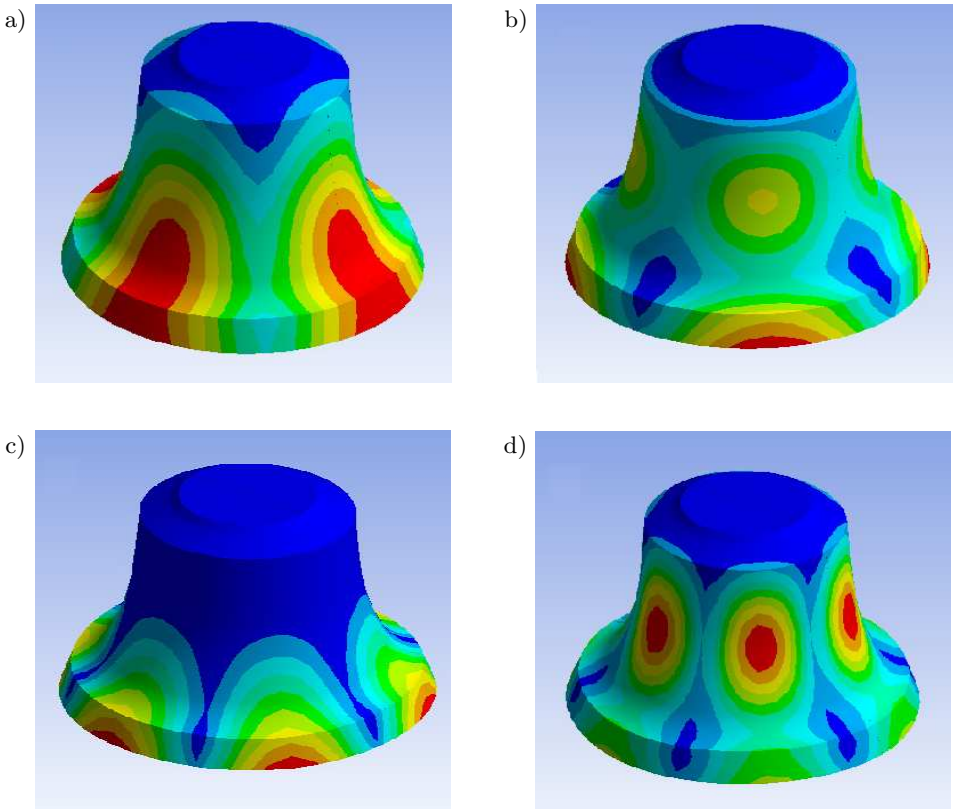

Fig. 5. Sigismund Bell mode shapes: a) first – hum (2,0), b) second – prime (2,1), c) third – tierce (3,0), d) fourth – quint (3,1).

the annular node line (2,1) in the second significant acoustic natural frequency, which does not happen in the case of bowls. According to Table 2, this allows for an addition in the sound spectrum of a component frequency approximately two times greater from the base frequency, which is a consonant octave interval. The introduced shape also causes the next mode shape (3,0) to contain a frequency 2.4 times higher than that of the base frequency, which is a minor third interval.

To ensure effective tuning of the acquired frequencies for them to fulfil the expected proportions per the DOE method (Mańczak, 1979) a digital experiment was planned. An extended *Central Composite Design* (CCD) plan was chosen (Myers, Montgomery, 2004) which features five levels of parameter changes. Upper and lower limits of the parameter values were set including the measured values of the actual bowls: height h $\in$ [0.064, 0.09] m, radius R $\in$ [0.045, 0.3] m, radius rg $\in$ [0.042, 0.047] m, thickness g $\in$ [0.0011, 0.0023] m. Figure 6 depicts the applied CCD plan for four normalised input variables.

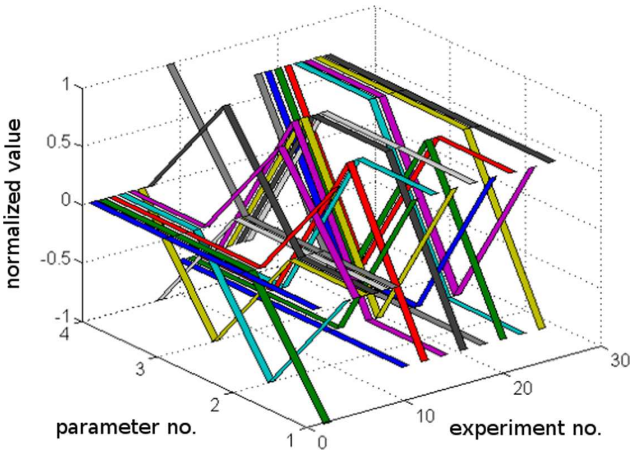

Fig. 6. Normalised experiment plan for four design parameters.

The proportions between the second, third, fourth, and fifth natural frequencies and the first frequency were assigned as the output parameters of the model. The response of the system described by use of a response hyper-surface was approximated by surfaces based on second-order polynomials, for which the overall form of the equation is given by:

$$\begin{aligned} y(x_1, x_2, ...x_N) = {} & a_0 + a_1x_1 + a_2x_2 + ... \\ & + a_Nx_N + a_{12}x_1x_2 + a_{13}x_1x_3 + ... \\ & + a_{23}x_2x_3 + a_{MN}x_Mx_N + a_{N+1}x_1^2 \\ & + a_{N+2}x^2 + ... + a_{N+N}x_N^2. \end{aligned} \tag{26}$$

Calculation of a_i, a_{ij} coefficients was carried out by the use of the regression analysis – approximation by the least square method (Mańczak, 1979). Exemplary response surfaces are depicted in Fig. 7, which, in this case, for the r and h parameters show their influence on the proportion changes between the second and first (p21) and the third and first (p31) frequencies of natural vibrations. It is worth noticing, that there is a visibly good agreement between marked with black squares design point values and values predicted by the response surface. The second observation is that for p31 parameter a design point in which the value reaches an integer number of 5 could be found, but it also makes it impossible for the p21 parameter. The tuning of model parameters was obtained by minimisation of the cost function. The defined cost function for m proportions between frequencies is in the form of:

$$\Phi = \sum_{j=1}^{m} \left(\frac{|y_j^* - y_j|}{y_{\max} - y_{\min}} \right), \tag{27}$$

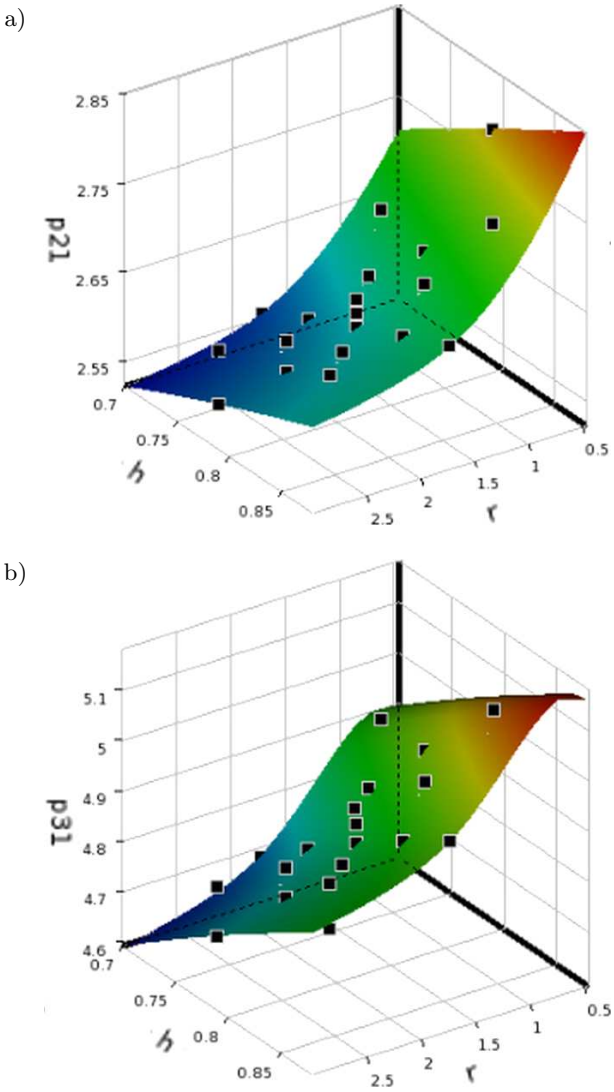

Fig. 7. Response surfaces for r and h parameter changes which contain natural frequency proportions of: a) second to first, b) third to first.

where $y_{\max}$, $y_{\min}$ are the maximum and minimum values on the response surface, y_j^* is the expected parameter, and y_j is the parameter obtained in the digital experiment.

Five parameters were chosen for the sound synthesis of the bell with appropriate lower and upper bounds of fi ∈ [0.69, 0.75] deg, gc ∈ [0.02,0.07] m, d ∈ [7.29, 7.51] m, ro ∈ [7600, 8800] kg/m-3, E ∈ [99, 121] GPa. The process of surface approximation corresponded to the one for the bowls.

3.2. Computation of the acoustic response

The acoustic response of the system (the changes in the sound pressure in the volume of air surrounding the vibrating structure) was determined by including Fluid30 acoustic elements (Fig. 8) to Shell281 surface elements in the case of bowls and to Solid186 solid elements in the case of bells. In accordance with the relations described in Subsec. 2.2, they use sound pressure as degrees of freedom. In addition, the acoustic elements in contact with the walls of the structure use node displacement as degrees of freedom as well. The external surface of the acoustic volume contained Fluid130 elements that took into account the condition of complete emission of sound from the system, which is the Sommerfeld radiation condition (Filipek, Wiciak, 2008; Gołaś, Filipek, 2009). It is implemented in semi-infinite elements and prescribes the asymptotic behaviour of the solution of wave equation in this exterior boundary value problem.

a)

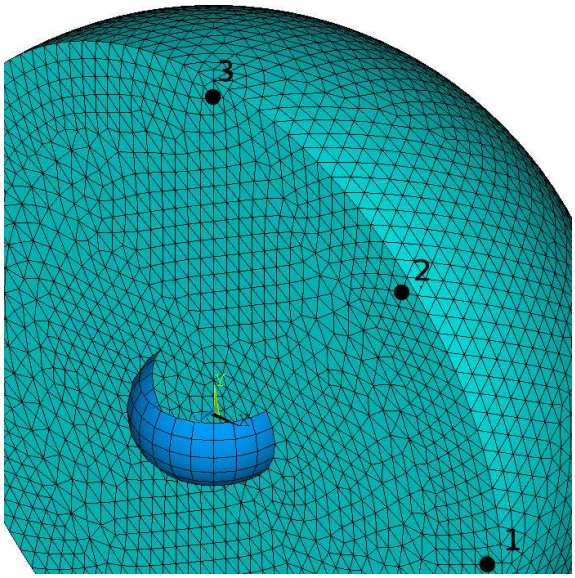

b)

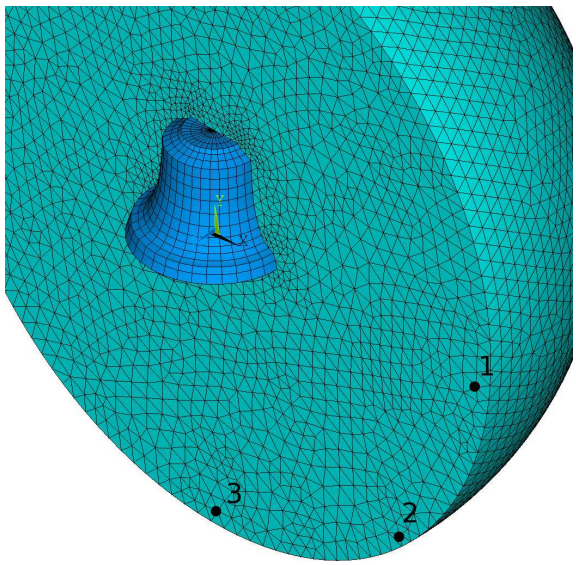

Fig. 8. Finite elements mesh including mechanical-acoustic coupling for: a) bowl, b) bell.

Both cases entailed a steady state analysis described in Eq. (25). The forcing in the system originated from a harmonic force applied to an element node. It was located on the edge of the bowl and on the internal wall surface of the bell, 0.02 m from the base. The amplitude of the force was 1 N and the frequency incrementally changed with a 1 Hz step from 2 to 4000 Hz for the bowl and from 2 to 400 Hz for the bell. Internal damping was introduced in the structure that was assumed to be constant in the whole range of frequencies, and was defined by using a damping coefficient of $2 \cdot 10^{-5}$.

Acoustic pressure changes were calculated for the whole acoustic volume, though this work includes the results for three selected points. In the case of bowls, they were 0.5 m away from the point of origin for the coordinates, and they were: point 1, on the intersection of the plane that is going through the bowl and the direction of force application; point 2, on the vertical plane at a 45 degree angle, and point 3, at a 90 degree angle on the bowl's axis. Analogous points were placed 3 m from the centre of the base of the bell. The sound pressure level and sound pressure phase angle regarding the force on the bowl are presented in Fig. 9a and Fig. 9b for the bell. Both systems indicate that the maximum sound pressure level is similar for acoustically important resonance frequencies. It varies from 2 to 12 dB between them. For the bell there is visible first resonance around 24 Hz for which the SPL is smaller than the next by more than 36 dB. It is associated with unrealistically rigid bell upper surface restraints and would definitely decrease after modelling the full crown of the bell or modification of the boundary conditions to a partly flexible characteristics with the use of lumped spring elements. It is also notable that amplitude frequency characteristics vary greatly with the change of the synthesis point and in both cases the measured levels for every resonance frequency are the lowest for the point located at the instrument axis. This is related to the directivity patterns that rely heavily on the mode shapes, and maximum sound pressure level is mostly in the direction perpendicular to the plane comprising the edge of the bowl or the base of the bell (Gołaś, Filipek, 2009).

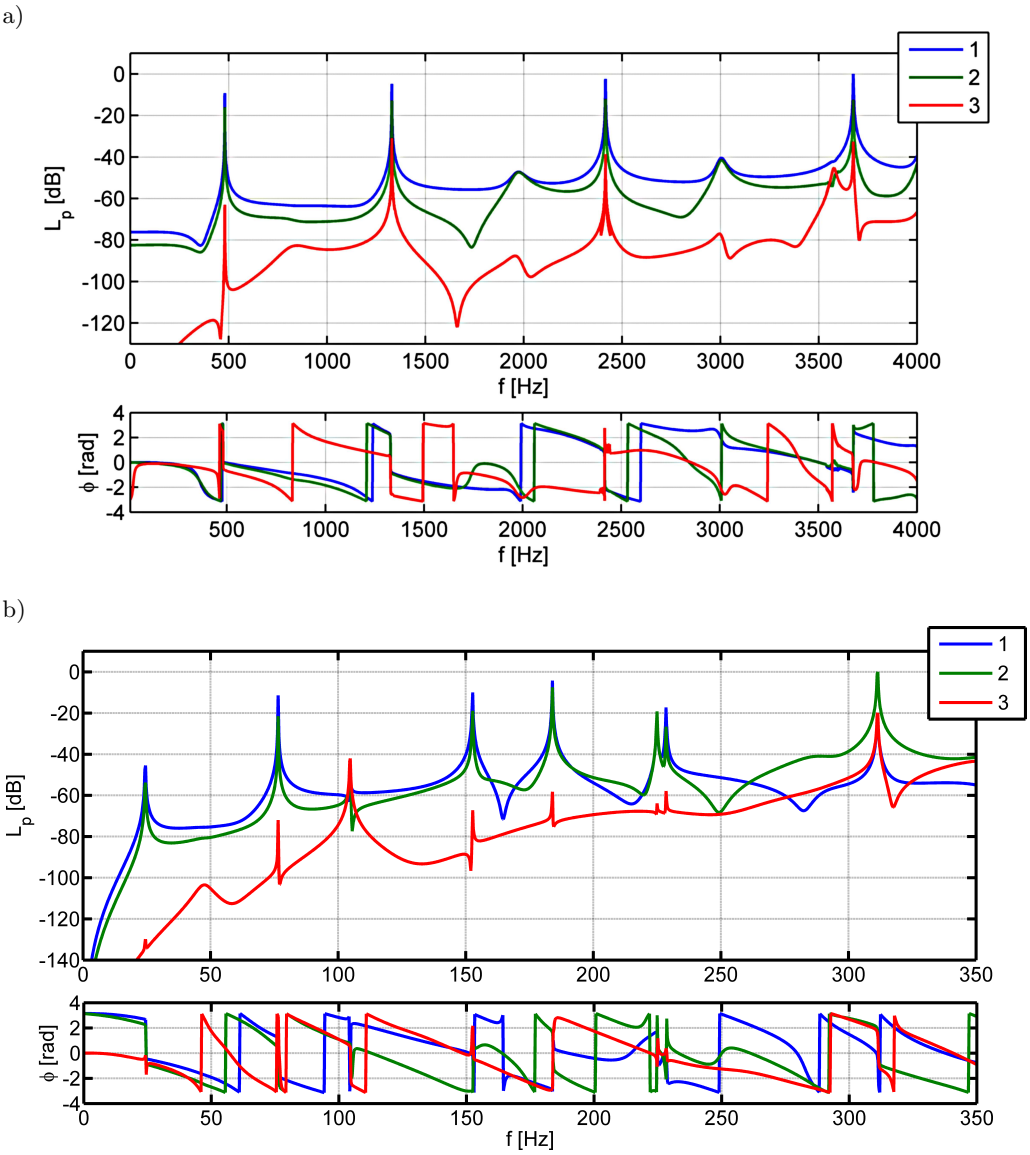

Fig. 9. Amplitude- and phase-frequency characteristic in selected points of the field for: a) Tibetan bowl no. 1, and b) Sigismund bell.

The waveform of the synthesised signal was obtained by using the methodology described in Subsec. 2.2. Spectral transfer function was assigned for three selected points as:

$$G_i(j\omega) = \frac{\widetilde{p}_i(j\omega)}{\widetilde{f}_S(j\omega)}, \quad i = 1, 2, 3. \tag{28}$$

With an assumption of the force $f(t)$ as a half-cycle sine pulse:

$$f(t) = \begin{cases} \sin(\omega t), & t \in [0, \pi/\omega] \\ 0, & t \notin [0, \pi/\omega] \end{cases} \tag{29}$$

the system response $p_i(t)$ was obtained by a convolution of an inverse Fourier transform of the system transfer function with the signal of the force:

$$p_i(t) = F^{-1}(G_i(j\omega)) * f(t). \tag{30}$$

The shape of the impulse in this synthesis was approximated as a half-cycle sine pulse, though it is worth noting that in the created synthesis method, the shape of the impulse may be approximated by any course, e.g., approximated on the basis of a signal acquired experimentally (Fletcher *et al.*, 2002) or by solving equations related to the movement of a bell-clapper system (Brzeski *et al.*, 2015) and approximating the force on the basis of collision modelling. The changes in the force signal flow do not influence the resonance frequencies occurring in the spectrum; they do, however, have an impact on the changes in their accompanying amplitudes.

To verify the universality of the used solutions based on the created meta-model, a synthesis of bowl sounds was carried out by assuming the expected proportions and making a compromise in tuning the con-

secutive components of the spectrum, and, in the case of bells, in defining the parameters for a bell of the same diameter as the Sigismund Bell with accurately tuned component frequencies of the spectrum 2:2.4:3:4. During the comparison of the appropriate signal pairs, it can be subjectively assessed what the influence of the applied corrections on the feeling of consonance is and how less unique would the Sigismund Bell sound be if it were to be precisely tuned.

4. Conclusions

The synthesis of the Tibetan bowls and bells' sound was carried out by a developed novel numerical synthesiser algorithm making use of the Design of Experiment (DOE) and Response Surfaces (RS) methods. The acoustic pressure signal was obtained by FEM calculations and further digital processing. This synthesizer when used on actual structures allowed obtaining a signal, the spectrum of which contains resonance frequencies very similar to the actual ones. It additionally allows for model parameter changes so that the listener could experience sound with a specific timbre.

The sound synthesis method presented in this work differs from the solutions used to date with the abstract synthesis, such as *additive*, *AM*, and *FM synthesis*, as the basis of this method is a mathematical model of an actual physical system including both surface vibrations and sound propagation in its vicinity. The proposed algorithm is an extension of physical instrument modelling methods. As a way of limiting the computational cost, which is an important aspect of their usage, methods such as *digital waveguide* synthesis are used (Czyżewski *et al.*, 1996; 2002), which are well-suited for simple shapes or simplifying assumptions related to the sound radiation. An often overlooked aspect is wavelength phenomena related to sound propagation in space. A direct numerical simulation conducted in the presented sound synthesis method is based on a model described by partial differential equations discretized by using FEM, which takes into account the full coupling of the mechanical and acoustic fields. Obtaining the system response in the time domain was carried out by an algorithm based on convolution of the force signal with the impulse response received by the way of spectrum transmittance. The approach presented in this work, never before seen in the field of sound synthesis, is based on carrying out a series of digital experiments and, additionally, building a metamodel of the system, allowing a reduction in the observation time of the influence of decision parameter changes on the spectrum of the obtained sound, which is possible by rapid readings and usage of results approximated by response surfaces.

The numerical synthesiser can be used for generating sounds of actual instruments as well as brand new ones, allowing for an analysis of the timbre of the instrument as early as at the planning stage. The synthesis resulted in a set of structural parameters which can be used while designing actual instruments. They can be also used during instrument restoration to assess the change in timbre caused by the modifications necessary during a repair.

References

1. Bilbao S. (2009), *Numerical sound synthesis: Finite Difference Schemes and Simulation in Musical Acoustics*, Wiley.
2. Brzeski P., Kapitaniaka T., Perlikowski P. (2015), *Experimental verification of a hybrid dynamical model of the church bell*, International Journal of Impact Engineering, **80**, 177–184.
3. Budzyński G., Sankiewicz M. (2000), *New Timbre of St. Catherine's Carillon*, Archives of Acoustics, **25**, 2, 147–155.
4. Cadoz C., Luciani A., Florens J.L. (1983), *Responsive input devices and sound synthesis by simulation of instrumental mechanisms*, Computer Music Journal, **8**, 3, 60–73.
5. Chih-Wei W., Chih-Fang H., Yi-Wen L. (2013), *Sound analysis and synthesis of Marquis Yi of Zeng's chime-bell set*, The Journal of the Acoustical Society of America, **133**, 5, 3590.
6. Czyżewski A., Jaroszuk J., Kostek B. (2002), *Digital waveguide models of the panpipes*, Archives of Acoustics, **27**, 4, 303–317.
7. Czyżewski A., Kostek B., Zieliński S. (1996), *Synthesis of organ pipe sound based on simplified physical models*, Archives of Acoustics, **21**, 2, 131–147.
8. Dobrucki A., Bolejko R. (2006), *FEM and BEM computing costs for acoustical problems*, Archives of Acoustics, **31**, 2, 193–212.
9. Fauvel J., Flood R., Wilson R.J. (2006), *Music and Mathematics: From Pythagoras to Fractals*, Oxford University Press.
10. Filipek R., Wiciak J. (2005), *Sound radiation of beam with shunted piezoceramics*, Archives of Acoustics, **30**, 4, 39–43.
11. Filipek R. (2013), *FEM application for synthesis of coupled vibroacoustic fields in a system with impulse excitation* [in Polish: *Zastosowanie MES do syntezy wibroakustycznych pól sprzężonych w układach o wymuszeniu impulsowym*], PhD Thesis, AGH University of Science and Technology.
12. Filipek R., Wiciak J. (2008), *Active and passive structural acoustic control of the smart beam*, The European Physical Journal – Special Topics, **154**, 1, 57–63.
13. Fletcher N.H., Rossing T.D. (1998), *The Physics of Musical Instruments*, Springer.
14. Fletcher N.H., McGee W.T., Tarnopolsky A.Z. (2002), *Bell clapper impact dynamics and the voicing of a carillon*, J. Acoust. Soc. Am., **111**, 3, 1437–1444.

15. Gołaś A., Filipek R. (2009), *Numerical Simulation for the Bell Directivity Pattern Determination*, Archives of Acoustics, **34**, 4, 407–419.

16. Gołaś A. (1995), *Computer methods in room and environmental acoustics* [in Polish: *Metody komputerowe w akustyce wnętrz i środowiska*, Wydawnictwa AGH.

17. Inácio O., Henrique L.L., Antunes J. (2006), *The Dynamics of Tibetan Singing Bowls*, Acta Acoustica United with Acoustica, **92**, 637–653.

18. Jiju A. (2014), *Design of Experiments for Engineers and Scientists*, Elsevier, London.

19. Lehr A. (1987), *A Carillon of Major-Third Bells, III. From Theory to Practice*, Music Perception, **4**, 267–280.

20. Lots I.S., Stone L. (2008), *Perception of musical consonance and dissonance: an outcome of neural synchronization*, J. R. Soc. Interface, **5**, 1429–1434.

21. McLachlan N., Keramati N.B. (2003), *The design of bells with harmonic overtones*, J. Acoust. Soc. Am., **114**, 505–511.

22. Mańczak K. (1979), *Methods for identifying the multidimensional control objects* [in Polish: *Metody identyfikacji wielowymiarowych obiektów sterowania*], Wydawnictwa Naukowo-Techniczne, Warszawa.

23. Myers R., Montgomery D. (2004), *Response surface methodology: A retrospective and literature survey*, Journal of Quality Technology, **36**, 1, 53–77.

24. Nowak Ł.J., Zieliński T.G. (2015), *Determination of the Free-Field Acoustic Radiation Characteristics of the Vibrating Plate Structures With Arbitrary Boundary Conditions*, Journal of Vibration and Acoustic, **137**, 051001.

25. Ren Z., Yeh H., Lin M.C. (2013), Example-guided Physically Based Modal Sound Synthesis, ACM Trans. Graph., **31**, 1, 1–16.

26. Rdzanek W.P. (2011), *Structural vibroacoustics of surface elements* [in Polish: *Wibroakustyka strukturalna elementów powierzchniowych*], Wydawnictwo Uniwersytetu Rzeszowskiego.

27. Rossing T.D. [Ed.], (2007), *Springer Handbook of Acoustics*, Springer Science & Business Media, LLC New York.

28. Smith J.O. III (1992), *Physical Modeling using Digital Waveguides*, Computer Music Journal, **16**, 4, 74–91.

29. Sankiewicz M., Kaczmarek A., Budzyński G. (1994), *Acoustic Investigation of the Carillons in Poland*, Archives of Acoustics, **19**, 3, 333–353.

30. Terwagne D., Bush J.W. (2011), *Tibetan singing bowls*, Nonlinearity, **24**, 51–66.

31. Zieliński T.P. (2005), *Digital signal processing* [in Polish: *Cyfrowe przetwarzanie sygnałów*], Wydawnictwa Komunikacji i Łączności, Warszawa.

32. Zienkiewicz O.C., Taylor R.L. (2000), *The Finite Element Method*, 5th Ed., Butterworth-Heinemann, Oxford.